

NPS ARCHIVE
1960
BURT, T.

INVESTIGATION OF HEAT TRANSFER
IN A VERTICAL ANNULUS

THOMAS E. BURT

DUDLEY KNOX LIBRARY
NAVAL POSTGRADUATE SCHOOL
MONTEREY CA 93943-5101

INVESTIGATION OF HEAT TRANSFER
IN A VERTICAL ANNULUS

by

Thomas E. Burt

Lieutenant, United States Navy

B.S

Submitted to the

Department of Mechanical Engineering

United States Naval Postgraduate School

Monterey, California

[1960]

NPS Archive

1960

Burt, T.

~~5/7/60~~

ABSTRACT

The heat transfer and pressure drop characteristics of water flowing in a vertical annulus under counter flow conditions were investigated. The heat exchanger used consisted of a straight tube in tube test section with water as the heat transfer medium in both tubes. Convection coefficients of heat transfer between the inner tube and the fluid flowing in the annulus were determined from the measured inner tube wall and average fluid bulk temperature and the energy transferred to the water flowing in the annulus.

The friction factor data indicate that the proper choice of diameter to be employed in evaluating the Reynolds number is the equivalent diameter, $d_e = (d_2 - d_1)$, and show that the transition from laminar to turbulent flow occurs at $Re \approx 2000$ as it does for flow inside tubes. The results for the laminar region are in excellent agreement with the theoretical predictions. Data in the turbulent region correlate well with that in the literature for commercial pipes.

The heat transfer data cover a range of Reynolds numbers from 200 to 5000. Two different types of runs were made: equal capacitance, (equal mass rate of flow in both tubes for this particular investigation) and constant wall temperature. The data indicate that the bulk temperature measurements were not reliable. However, since the measured temperature differences were reliable, it was possible to correlate both laminar and turbulent flow data by one empirical equation. The bulk temperature distribution for the constant wall temperature run along the annulus length was found to have a large effect on the heat transfer coefficients. It is not linear and should be taken into account. The

data were best correlated by evaluating fluid properties at an average film temperature rather than an average bulk temperature as recommended in most of the literature.

ACKNOWLEDGEMENT

The author is indebted to Professor Charles P. Howard for suggesting the investigation of vertical annular flow and for his interest, advice and patience during the progress of the work.

TABLE OF CONTENTS

Title	Page
Abstract	i
Table of Contents	iii
List of Tables	iv
List of Figures	v
List of Symbols	vi
I. Introduction	1
II. Description of Equipment	2
III. Experimental Procedures	4
IV. Experimental Results	6
V. Sources of Error	8
VI. Discussion of Results	10
VII. Conclusions and Recommendations	17
Bibliography	19

LIST OF TABLES

TABLE		Page
1	Summary of Apparatus Dimensions	20
2	Isothermal Friction Data	21
3	Heat Transfer Data	22

LIST OF FIGURES

Figure		Page
1.	Details of heat exchanger construction.	24
2.	Schematic wiring diagram of thermocouple circuitry.	25
3.	Details of traveling thermocouple design.	26
4.	Details of traveling thermistor design.	27
5.	Schematic of the overall test assembly.	28
6.	f versus Re .	29
7.	Nu_{am} vs $(Re)^{.45} (Pr)^{.5} (Gr)^{.05} (\mu_b/\mu_1)^{.14} (de/L)^{.4} (d_2/d_1)^{.8}$	30
8.	Nu vs $(Re)^{.8} (Pr)^{.33} (d_2/d_1)^{.53}$	31
9.	Nu vs $(Re)^{.8} (Pr)^{.5} (Gr)^{.05} (\mu_b/\mu_1)^{.14} (de/L)^{.4} (d_2/d_1)^{.8}$ for all laminar runs with parameters based on average bulk temperatures and fluid properties evaluated at an average film temperature.	32
10.	Nu vs $(Re)^{.58} (Pr)^{.645} (Gr)^{.065} (de/L)^{.516} (d_2/d_1)^{.027}$ for all runs.	33
11.	Dimensionless plot of temperature versus annulus length for run 7.	34
12.	Dimensionless plot of temperature versus annulus length for run 20.	35
13.	Dimensionless plot of temperature versus annulus length for run 28.	36
14.	Dimensionless temperature versus diameter for laminar and turbulent flow in a tube.	37
15.	Calibration curve for the thermistor.	38
16.	Dimensionless temperature versus length for the constant wall temperature runs.	39
17.	$St(Pr)^{2/3}$ versus Re .	40

LIST OF SYMBOLS

English Letter Symbols

A	Area (ft^2).
c	Specific heat ($\text{BTU}/\text{lbm}^\circ\text{F}$).
C	Capacitance ($\dot{m} c_p$)
d	Diameter (ft.)
de	$d_2 - d_1$ (ft)
f	Friction factor $(\Delta p/p) d_e / 2 L u^2$
g	Acceleration of gravity ($32.2 \text{ ft}/\text{sec}^2$)
G	\dot{m}/A ($\text{lbm}/\text{hr. ft}^2$)
h	Convective coefficient of heat transfer ($\text{BTU}/\text{hr. ft}^2.^\circ\text{F}$).
k	Thermal conductivity ($\text{BTU}/\text{hr. ft } ^\circ\text{F}$).
L	Length (ft.).
\dot{m}	Mass rate of flow ($\text{lbm}/\text{hr.}$)
p	Pressure ($\text{lb}_f/\text{in.}^2$)
Q	Heat transfer per unit time ($\text{BTU}/\text{hr.}$)
r	Radius (ft.)
t	Temperature ($^\circ\text{F}$)
u	Velocity ($\text{ft.}/\text{sec.}$)
x	Length (ft.)

Greek Letter Symbols

Δ	Difference
μ	Viscosity ($\text{lbm}/\text{ft. sec.}$)
ρ	Density (lbm/ft^3)
ϕ	Function of
β	Coefficient of thermal expansion ($1/^\circ\text{R}$)

Subscripts

a	Inner pipe wall
am	Arithmetic mean
b	Bulk value
c	Annulus fluid
f	Film value
h	Pipe fluid
i	Inlet
n	Average value
o	Outlet
p	Constant pressure
1	Inner annulus wall
2	Outer annulus wall

Dimensionless Groups

Gr	Grashof number	$(g \beta p^2 \Delta t d_e^3 / \mu^2)$
Nu	Nusselt number	$(h d_e / k)$
Pr	Prandlt number	$(c_p \mu / k)$
Re	Reynolds number	$(d_e G / \mu)$
St	Stanton number	$(h / \rho u c_p)$

I Introduction.

The problem of heat transfer in annular spaces has not been adequately solved and is complicated by the many forms in which the empirical correlation equations are presented, [3], [4], [5].* Although a number of equations relating convection heat transfer coefficients to system parameters have been presented in recent years, [1], [2], these provide correlations only for selected ranges of the pertinent variables. The development of proper relations for predicting annular heat transfer is made difficult, not only by an almost complete lack of data in the laminar region [14], but also by insufficient data covering both laminar and turbulent flow in the same annulus.

It has been the objective of this investigation to obtain (1) friction data for water flowing in the annulus of a vertical double tube heat exchanger over a range of Reynolds number 180 to 8000 and (2) heat transfer data for the same annulus over a range of Reynolds number 200 to 5000 which was the limit of the equipment. The purpose of the friction data was to determine the proper characteristic length to be utilized in evaluating the Reynolds number. The heat transfer results were treated in a manner to bring out their comparison with existing empirical correlations, and to establish a correlation which would cover the transition Reynolds number range.

(*) Numbers in brackets refer to the Bibliography on page 19.

II. Description of Equipment.

Heat Exchanger. The heat exchanger proper consisted of a single vertical 1.125 inch O. D. x 0.995 inch I. D. 99.9% copper tube inside a 1.372 inch O. D. x 1.242 inch I. D. 99.9% copper tube 142 inches long. The annular diametric clearance was 0.117 inches and was maintained by a helical arrangement of 36 stainless steel ball bearings, 0.093 inch diameter, imbedded in the inner tube wall and fastened by solder. Details of construction are shown in Figures 1 and essential dimensions in Table 1

Certain aspects are worthy of comment. The annular space was made sufficiently small so that reasonable annulus water velocities might be obtained at low mass rates of flow. Inlet and outlet header spaces were made sufficiently large to permit proper measurement of the bulk temperatures. Copper-constantan immersion thermocouples were used to measure the inlet and outlet temperatures of both streams. A switch was built which enabled both absolute temperatures and temperature differences to be read. A schematic wiring diagram of the switching arrangement is shown in Figure 2. The circuit was designed to eliminate the interference from the circulating circuits existing between all the thermocouples. On the outer annulus tube 36 copper-constantan thermocouples were anchored by soldering in 1/32 inch holes drilled half way through the tube wall. These were placed in groups of three, equally spaced around a diameter, at 11 inch intervals down the length of the tube. The inside wall temperature of the inner tube was measured by means of a "traveling" thermocouple. Several designs were used and Figures 3 and 4 show the details of construction. A Victory Corporation 2000 ohm

glass enclosed thermistor was used for one design of the "traveling" thermocouple. It was calibrated in water with all leads in place and the calibration curve is shown in Figure 15.

Pressure taps were drilled in the outer tube at a distance of 21 inches from each end giving a distance of 100 inches between taps. Both mercury and water manometers were used to measure pressure drop. For reading the small pressure differentials a Fisher cathetometer was used which read to the nearest 0.01 centimeter.

Auxiliary Equipment. The overall test assembly is shown in Figure 5. A large hot water storage tank provided a heat reservoir of uniform temperature. The water was not changed during the investigation, therefore assuring a minimum of entrapped gasses and particles in the circuit. Fischer and Porter Flowrator meters were used to measure the flow rates for both hot and cold systems. These also served to indicate stability of the flow. The 36 outer wall thermocouple readings were taken with a Minneapolis - Honeywell 48 position recording potentiometer. These readings were recorded to a precision of $\pm 0.2^{\circ}\text{F}$. All other thermocouples were read with a portable precision hand balance Rubicon potentiometer which was accurate to the nearest $\pm 0.1^{\circ}\text{F}$. The thermistor resistance was read with a wheatstone bridge balancing arrangement and was accurate to the nearest $\pm 0.1^{\circ}\text{F}$.

The heat exchanger proper was wrapped with 2 inch width asbestos cloth and then covered with 1 1/2 inch thick pipe lagging.

III. Experimental Procedure.

Friction: To obtain isothermal friction data, pressure drop measurements were made of the fluid flowing in the annular space at various flow rates. The pressure taps were so located to give an entrance length of 180 equivalent diameters. Pressure differences of less than 50 inches of water were determined with a water manometer using a cathetometer to secure accurate readings. For pressure differences of 50 inches of water or more a mercury manometer was used. The water temperature for most of the runs was essentially room temperature. Five check runs were made at a temperature of 100°F. For low flow rates an electric timer and a weighing tank were used to determine the mass rate of flow. These measurements were used to check the calibration of the flow meters. At low flow rates the flow meter measurements varied as much 6% with the flow rate obtained by weighing, but the overall variation was less than $\pm 2\%$.

Heat Transfer: The procedure for the equal capacitance runs and the constant wall temperature runs was essentially the same. For equal capacitance, the mass flow rates in the annulus and inner tube were kept the same since the specific heat for water was constant over the temperature range employed. Flow rates for the annulus were varied to cover a Reynolds number range of 200 to 5000.

For constant wall temperature runs the inner tube mass flow rate was held constant at as high a value as permitted by the apparatus, corresponding to a Reynolds number of about 11,000 for all runs. For the annulus, the mass flow rate was varied to correspond to a range of Reynolds number of 200 to 2800.

The hot water temperature was controlled by rheostats on the heaters and the energy input measured by a voltmeter and ammeter. For the hot water circulating system sufficient cold make-up water was added to keep a constant water level in the reservoir.

Data for the runs were taken after five to ten minutes of steady state operation of the system. Steady state conditions were denoted by the constancy of flow rates and temperatures and were usually reached within an hour after changes in operating conditions had been made. Repeat data recordings were made of all temperatures except those of the "traveling" thermocouple.

The inner tube wall temperatures were determined by moving the "traveling" thermocouple up or down the tube in 12 inch increments.

IV. Experimental Results.

The friction results are shown in Figure 6 and tabulated in Table 2. The table also presents the temperatures, pressure differences and flow rates for the individual runs.

The heat transfer results are shown in Figures 7, 8, 9, 10 and 17 and tabulated in Table 3. The table also presents the temperatures, flow rates and all other data used to calculate the system parameters as well as the parameters themselves. Inner wall temperatures were not corrected for thermocouple error as calculations of the temperature difference introduced by the exposed wires, using Schneider's flat plate analogy [6], showed this effect to be insignificant.

The inner wall temperatures were corrected according to laminar or turbulent flow in the inner tube for the physical distance of the thermocouple from the inner wall. This distance was 0.02 inches and amounted to 4% of the tube radius. Figure 14 shows Martinelli's [16] and Eckert and Drake's [15] temperature profiles for turbulent and laminar flow respectively. A value of 0.625 was used for turbulent flow calculations and a value of 0.15 for laminar flow calculations. A correction to account for the temperature drop across the inner tube wall was also made. The value of thermal conductivity, k , for pure copper of 220 BTU/hr.ft. $^{\circ}$ F was used. This value is probably slightly high as the tube is only 99.9% pure copper.

The average bulk temperatures of the annular fluid for constant wall temperature runs were corrected to account for the temperature distribution with annulus length. The three thermocouple readings at each of the 12 outside annulus wall positions were averaged and a

dimensionless temperature, $t_x - t_{ci} / t_{co} - t_{ci}$, was computed for each position. Simpsons Rule was used to calculate an average bulk temperature for each run. The average inner annulus wall temperatures were determined by an arithmetic average of the end wall temperatures.

For the equal capacitance runs both the inner and outer annulus wall temperature distributions were considered linear and the average wall and average bulk temperatures determined on that basis.

The system parameters are based on a film value temperature, t_f , defined as

$$t_f = t_{in} + t_{bcn} / 2 \quad (1)$$

The data were also correlated using bulk temperatures and an average bulk temperature as a basis for calculating system parameters.

V. Sources of Error.

The temperature measurement technique offered the principal chance for error and all numerical results were a direct consequence of these. To minimize these errors, all thermocouples for bulk temperature measurements were similar and all manufactured thermocouples came from the same spool of wire and were made by the same method. A circuit arrangement, Figure 2, was built to eliminate circulating current effects. Measured differences rather than absolute temperature measurements were used whenever possible. All readings were made on the same potentiometer and referenced against the same standard cell.

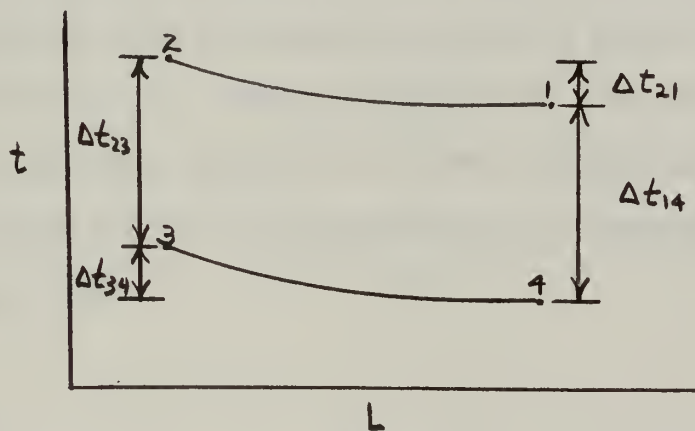


Figure A.

As shown in Figure A, the sum of $\Delta t_{21} + \Delta t_{14}$ should equal the sum of $\Delta t_{23} + \Delta t_{34}$. These measured temperature differences were totaled and found to vary an average of 2.5%. This indicates the circuit design eliminated the circulation errors.

The sensitivity of the potentiometer was $\pm .001$ millivolt or approximately $\pm 0.04^\circ\text{F}$. Conversion of millivolts to degrees Fahrenheit was done from Leeds and Northrup Conversion Tables for Thermocouples.

Flow rate variation was a second potential source of error. The flow meter readings were checked during the friction test by weighing the mass of water for a given time. The flow meters are considered accurate to $\pm 2\%$. At least five readings were taken for each run and they did not vary more than 1%.

Further sources of error which were determined to be insignificant included (a) expansion or contraction of the annulus tubes with temperature fluctuations, (b) variation of the temperature during the time required for observation, (c) heat loss along the thermocouple wire and (d) the bi-metallic thermoelectric effect at the connector terminals. The latter connectings were designed and located to insure that both connections for each thermocouple lead would remain at the same temperature thus assuring no effect on the results from this extra junction.

An uncertainty analysis of the above effects on the system parameters indicates that the repeatability of experimental data should be within $\pm 10\%$.

VI. Discussion of Results.

Friction: The isothermal friction data shown in Figure 6 are plotted as friction factor versus Reynolds number, based on an equivalent diameter. The change from laminar to turbulent flow is seen to occur approximately at a Reynolds number of 2000 which corresponds to the critical value for transition of flow inside tubes [10]. As it is desirable for comparison purposes to have the critical value of Reynolds number which conforms with that of flow in tubes, it was decided the equivalent diameter was the preferred characteristic defining length.

As shown by Lamb [7], besides the usual relations for friction factor,

$$f = \frac{(\Delta p / \rho) d_e}{2 u^2 L}, \quad (2)$$

and Reynolds number,

$$Re = \frac{d_e G}{\mu}, \quad (3)$$

for flow of fluids in an annulus an additional geometry parameter,

$$\phi(d_1/d_2) = \frac{(1 - d_1/d_2)^2}{1 + (d_1/d_2)^2 + \frac{[1 - (d_1/d_2)^2]}{\ln(d_1/d_2)}}, \quad (4)$$

is needed. The limits of $\phi(d_1/d_2)$ being

$$\phi(d_1/d_2) = 1 \quad \text{when } d_1/d_2 = 0$$

as for flow in tubes, and

$$\phi(d_1/d_2) = 1.5 \quad \text{when } d_1/d_2 = 1$$

as for flow between parallel plates. The functional relationship between the parameters for laminar flow is theoretically found to be

$$f = \frac{16}{Re} \phi(d_1/d_2). \quad (5)$$

For the annulus used in this investigation

$$\phi(d_1/d_2) = 1.499 \simeq 1.5,$$

giving a theoretical prediction of the friction factor for laminar flow as

$$f = \frac{24}{Re}. \quad (6)$$

From Figure 6 it is seen that the experimental values of the friction factor are within $\pm 5\%$ of the theoretical values over a Reynolds number range of 200 to 2000.

In the turbulent flow region, ($Re > 2000$), the data were plotted and correlated by the equation:

$$f = 0.0366 (Re)^{-0.2} \phi(d_1/d_2). \quad (7)$$

These data plot 12% higher than the proposed equation of Knudsen and Katz [8] of:

$$f = 0.076 (Re)^{-0.25}, \quad (8)$$

and 6.5% higher than the proposed Davis [9] relationship:

$$f = 0.055 (Re)^{-0.2} \left(\frac{d_2/d_1 - 1}{d_2/d_1} \right)^{0.1} \quad (9)$$

The correct function of the Reynolds number to use appears to be $(Re)^{-0.2}$ as the slope of the line in Figure 6 is -0.2. Equation (8) expresses the friction factor by taking the average of a number of investigators' experimental results [8] and neglects to account for any function of diameter. Knudsen and Katz [8] predict a 35% variation from equation (8), depending on the ratio of (d_2/d_1) . Only for larger (d_2/d_1) ratios, above 3, may equation (8) be used with small error. It is, therefore, recommended that the Davis equation be used, especially for small values of (d_2/d_1) . It is noted that the turbulent data fall very close to the line for flow inside commercial pipes.

Heat Transfer. Figure 7 is a plot of all the laminar flow data correlated by using the Chen, Hawkins and Solberg [11] equation based on the arithmetic mean bulk temperature of the fluid and the viscosity,

μ_i , evaluated at the inner annulus wall temperature t_{in} :

$$Nu_{am} = 1.02 (Re)^{.45} (Pr)^{.5} (Gr)^{.05} (\mu_b/\mu_i)^{.14} (d_e/L)^{.4} (d_2/d_1)^{.8} \quad (10)$$

The data fall an average of 30% below the empirical curve.

For the turbulent equal capacitance runs, Monrad and Pelton's [12] equation based on the average fluid bulk temperatures,

$$Nu = .020 (Re)^{.8} (Pr)^{.33} (d_2/d_1)^{.63} \quad Re > 10,000, \quad (11)$$

was used and a plot is presented in Figure 8. The turbulent data fall 50% below the empirical curve.

The lack of correlation between these data and the empirical equations is obvious. The main explanation lies in the fact that the measured bulk

temperatures were not true temperatures. The mixing chambers did not perform properly and further, the inner pipe conducted heat into both annuli mixing chambers, which would also contribute to bulk temperature error. This is substantiated by comparing the hot and cold bulk temperature readings at the ends of the annulus. The cold water inlet temperature which should remain fairly constant rises and falls with a hot water temperature rise and fall.

The hot water bulk temperature measurements are considered better than the cold water bulk temperature measurements because the thermocouples could be placed nearer the center of the tube. The cold water bulk thermocouples could not be placed closer than the outside radius of the inner tube and, therefore, could be considerably influenced by conduction from the hot tube as well as not actually "seeing" the inlet or outlet cold water temperatures. The inner and outer annulus wall temperatures are considered good as well as the bulk temperature differences.

Another possible reason for the discrepancies with these correlations is due to the effect of natural convection. There are no correlations in the literature that cover the flow conditions for the particular annulus investigated. In general, natural convection is expected to influence the heat transfer behavior in an amount of $\pm 15\%$ depending on its relation to the external forces [13]. For the Chen, Hawkins and Solberg correlations with the Grashof number raised only to the 0.05 power, practically all of the free convection effects are damped out. In the Monrad and Pelton correlation no free convection effects are included since, with Reynolds numbers in excess of 10,000, the inertia forces

completely override the buoyant forces.

It was found that all of the data of this investigation, including the transition Reynolds number range, could be correlated by the equation

$$\text{Nu} = 0.093 (\text{Re})^{.58} (\text{Pr})^{.45} (\text{Gr})^{.065} (d_e/L)^{.516} (d_2/d_1)^{1.027} \quad (12)$$

a plot of which is presented in Figure 10. This equation correlated all data with an average variation of $\pm 10\%$ and a maximum variation of 20%. The Sieder and Tate [17] viscosity correlation, (μ_b/μ_f) , is not included as it is recognized that the present data do not cover a sufficient variation in temperature gradient to test this relationship, and also previous investigations have not been sufficiently extensive to prove this effect [2]. The parameters of equation (12) are evaluated at a film temperature defined by equation (1). The use of a film temperature allows for variations of all physical properties and resulted in the best correlation by an empirical equation.

For equal capacitance laminar runs, the inner wall temperature correction for thermocouple location was made using Martinelli's [16] turbulent temperature distribution rather than the laminar temperature distribution. This was done because it gave the best correlation of these data with respect to constant wall temperature data and the turbulent equal capacitance data.

Figures 11, 12, 13, and 16 are dimensionless plots of annulus wall temperatures versus annulus length, and show that for the flow conditions of this investigation the temperature distributions are definitely not linear. However, it is believed that the arithmetic mean of the fluid bulk temperature is a close approximation to the average fluid temperature for equal capacitance runs. The arithmetic mean bulk temperature

for the constant wall temperature runs was found to vary as much as 25% from the average bulk temperature as found by applying Simpson's Rule. It is recommended that the average bulk temperature be used to evaluate the heat transfer as well as the film temperature for evaluating fluid properties. The average bulk temperature for the constant wall temperature runs was found to be

$$t_{bcn} = .673 \Delta t_{bc} + t_{bci}, \quad (13)$$

and is recommended for use where knowledge of the bulk temperature distribution is unknown.

All of the laminar runs were also correlated using the Chen, Hawkins and Solberg equation (10) but basing the fluid properties on a film temperature and using the above average bulk temperature, equation (13). These data plot an average of 15% higher than predicted by equation (10). A plot is shown in Figure 9.

A final correlation was made for all runs based on the Colburn analogy [19] of

$$St (Pr)^{2/3} = \phi (Re) \quad (14)$$

with the fluid properties evaluated at the film temperature, equation (1). These results are shown in Figure 17. While it was expected that the Colburn analogy would produce an acceptable curve for the fixed geometry of the system and counter flow fluid arrangement, it was indeed startling to find the small scatter of the data and the straight line behavior exhibited. It can only be postulated from the correlation that for the Reynolds number range covered and the small temperature differences which were employed, natural convection effects for all of the runs must

have been of the same order of magnitude. Any attempt to introduce the Grashof number into the correlation merely scattered the data, thus indicating the free convection effects were negligible. The extrapolated conclusion can be only that for a certain range of diameter ratios and equivalent diameters, even for laminar flow conditions, the Grashof number is not a pertinent parameter.

VII. Conclusions and Recommendations.

The friction data indicate that the proper Reynolds number to employ is deG/μ , where de is the equivalent diameter of the annulus. The friction data in the laminar region check the theoretical relation of Lamb [7] and this should be employed for annuli in this region of flow.

The heat transfer data, both laminar and turbulent, were correlated by equation (12) based on the average bulk temperature and the fluid properties evaluated at a film temperature defined by equation (1). This equation is presented as being valid only for use in investigating this particular geometry annulus and for identical conditions of flow. It is also suggested that equation (12) is valid for both heating and cooling.

There is to date no single empirical correlation which can account for all the possible variations of flow conditions and annuli geometry. If knowledge of the heat transfer within $\pm 5\%$ is needed, then a particular correlation must be found in the literature that applies to the specific type of flow pattern and annuli geometry under investigation.

It would be interesting to know exactly how natural convection effects the heat transfer in vertical annuli. This could be found by reversing the direction of flow in the annulus and tube and analyzing the effect. It has to be expected that for large Reynolds numbers and small Grashof numbers, the influence of free convection on the heat transfer can be neglected. At what point this occurs is yet to be determined. The Grashof number varied as much as 200% over the range of Reynolds numbers investigated. The Grashof number enters into equation (10) to the 0.05 power only and as such varied less than 2% over the range of

Reynolds numbers investigated. However, if the Grashof number enters into the correlation to the 0.065 power as in equation (12), it will produce a 12% variation over the range of Reynolds numbers investigated. This agrees with Eckert and Diaguila's [18] prediction of a 10% variation in the heat transfer due to natural convection effects. An account must be made as to how the buoyancy forces act in conjunction with the external forces. A variation of 10% in the Nusselt number would result from ignoring this fact.

BIBLIOGRAPHY

1. Wm. H. McAdams, Heat Transmission, McGraw-Hill Book Company, Inc., (1954) p. 243.
2. R. P. Stein and Wm. Begell, Heat Transfer to Water in Turbulent Flow in Internally Heated Annuli, Journal AIChE, 4; p. 127, (1958).
3. J. H. Wiegand, Discussion of Paper by McMillen and Larson, Trans. AIChE, 41; p. 147 (1945).
4. M. Jakob and K. A. Rees, Trans. AIChE, 37; p. 169, (1941).
5. R. H. Norris and M. W. Sims, Trans. AIChE, 38; p. 469, (1942).
6. P. J. Schneider, Conduction Heat Transfer, Addison - Wesley Publishing Company, Inc., 1st Ed., p. 176, (1955).
7. H. Lamb, Hydrodynamics, Cambridge University Press, London, 5th Ed., p. 555, (1924).
8. Knudsen and Katz, Fluid Dynamics and Heat Transfer, McGraw-Hill Book Company, Inc., 1st Ed., p. 383, (1958).
9. E. S. Davis, Trans. Amer. Soc. Mech. Engrs., 65; p. 759, (1943).
10. E. S. Davis, Trans. Amer. Soc. Mech. Engrs., 65; p. 198, (1943).
11. Chen, Hawkins and Solberg, Trans. ASME, 68; p. 99, (1946).
12. C. C. Monrad and J. F. Pelton, Trans. AIChE, 38; p. 593, (1942).
13. F. Krieth, Principles of Heat Transfer, International Textbook Company, 1st Ed., p. 336, (1958).
14. F. G. Carpenter, A. P. Colburn and E. M. Schoenborn, Trans. AIChE, 42; p. 165, (1946).
15. E. R. G. Eckert and R. M. Drake Jr., Heat and Mass Transfer, McGraw-Hill Book Company, Inc. 1st Ed., p. 195, (1959).
16. R. C. Martinelli, Trans. ASME, 69; p. 947, (1947).
17. E. N. Sieder and G. E. Tate, Ind. Eng. Chem., 28: 1429-35 (1936).
18. R. G. Eckert and A. J. Diaguila, Trans. ASME, 76; (1954).
19. A. P. Colburn, Trans. Am. Inst. Chem. Engrs, 29; 174-209 (1933).

Table I. Apparatus Dimensions

Inner Tube: 1 inch I. D. x 20 foot Copper Tube

Effective tube length - 142 inches - 11.82 feet

Diameter (inside) - 0.995 inches - 0.0825 feet

Diameter (outside) - 1.125 inches - 0.0948 feet

Wall Thickness - 0.065 inches

Cross-Sectional Area (inside) - 0.00498 square feet

Circumference (outside) - 0.29437 ft.

Effective Heat Transfer Surface (outside) - 3.48 square feet

Jacket Tube:

Diameter (inside)-1.242 inches - 0.1035 feet

Diameter (outside) - 1.3 1/2 inches - 0.1143 feet

Cross Sectional Area (inside)- 0.3143 feet

Circumference (inside)- 4.46 inches - 0.372 feet

Annulus:

Equivalent Diameter: 0.117 inches - 0.00976 feet

Cross-sectional Area - 0.00151 feet

Effective friction length - 100 inches - 8.33 feet

TABLE II

Isothermal Friction Data

Flow rate lbm/sec.	t °F	$\Delta p/p$ cm lbf/lbm	u $\frac{\text{lbm}}{\text{ft} \cdot \text{sec}} \times 10^3$	u ft/sec	f	Re
0.0208	64	8.16	0.716	0.221	0.108	187
0.0258	65	11.20	0.705	0.274	0.0921	236
0.0361	63	16.55	0.725	0.383	0.0696	322
0.0450	62	20.64	0.736	0.477	0.0572	395
0.0548	64	25.16	0.716	0.582	0.0457	495
0.0665	64	29.88	0.716	0.705	0.0371	600
0.0826	63	38.18	0.725	0.876	0.0307	736
0.0945	64	42.53	0.716	1.005	0.0259	853
0.1122	62	52.7	0.736	0.190	0.0229	985
0.1293	62	58.7	0.736	1.372	0.0192	1135
0.1367	64	62.7	0.716	1.448	0.0184	1232
0.1412	62	69.0	0.736	1.498	0.0189	1240
0.1823	61	95.3	0.747	1.932	0.0157	1575
0.3152	62	201	0.736	3.33	0.0113	2760
0.371	62	283	0.736	3.94	0.0111	3260
0.494	60	453	0.759	5.24	0.0102	4200
0.569	58	587	0.780	6.04	0.00995	4720
0.674	57	800	0.791	7.15	0.00965	5500
0.751	57	978	0.791	7.97	0.00951	6130
0.0411	98	12.95	0.460	0.438	0.0415	578
0.0807	98	24.82	0.460	0.862	0.0209	1132
0.145	99	46.2	0.460	1.550	0.0118	2030
0.338	99	196	0.463	3.61	0.00927	4320
0.409	99.5	276	0.463	4.36	0.00895	5690
0.533	99.5	460	0.467	5.69	0.00883	7360
0.576	99.5	574	0.467	6.16	0.00932	7960

TABLE III
Equal Capacitance Runs

Run	\dot{m} lb/hr	t_{bhi} °F	t_{bho} °F	t_{bco} °F	t_{aci} °F	t_{bci} °F	t_{aci} °F	t_{bci} °F	$\frac{h}{h_{e-fc=0.5}}$ BTU/hr-ft ² -°F	Nu	$\frac{Q}{h_{e-fc=0.5}}$ BTU/hr	Re	St	Fig. A Temp. Variation %
7	2250	77.2	70.0	66.0	75.7	58.9	75.7	62.5	612	17.4	15750	5830	441	+1.3
8	2300	76.4	69.0	66.2	75.8	58.3	75.8	62.6	650	18.5	16550	5970	426	-1.0
9	2080	76.5	68.4	65.8	75.6	57.3	75.6	61.2	555	15.7	16200	5330	405	-2.4
10	1825	77.6	69.0	65.5	74.9	56.3	74.9	60.5	546	15.5	15180	4740	437	-2.4
11	1725	77.5	69.5	64.5	73.3	56.7	73.3	60.5	562	15.9	13290	4320	487	+3.9
12	1575	78.2	69.5	65.5	74.8	57.3	74.8	61.3	489	14.2	12750	4040	474	+1.3
13	1396	77.9	70.1	66.5	74.6	59.7	74.6	63.1	471	13.3	10050	3600	508	+5.7
14	1250	78.7	70.8	66.9	76.4	59.6	76.4	63.3	425	12.0	9520	3280	536	+2.1
15	1095	79.4	71.2	68.0	75.9	59.6	75.9	63.5	436	12.3	8550	2880	588	0.0
16	951	78.0	70.3	67.9	73.7	60.2	73.7	63.8	410	11.4	6850	2470	635	+4.1
17	805	77.9	70.4	67.3	75.7	60.6	75.7	65.9	331	9.35	5640	2120	628	+5.9
18	676	78.3	71.0	69.5	75.4	62.1	75.4	66.6	248	7.00	4940	1860	556	+4.2
19	527	78.9	71.4	70.8	73.4	62.6	73.4	66.1	208	5.85	3840	1430	595	+2.8
20	375	79.2	72.9	70.2	73.6	63.9	73.6	67.0	251	7.07	2360	1020	1010	+1.7
21	275	80.1	72.8	70.4	73.5	63.3	73.5	66.9	193	5.45	1950	750	1029	+1.3
22	257	79.0	73.2	70.9	73.3	65.2	73.3	68.1	166	4.66	1390	706	1078	+3.8
23	238	79.8	73.6	73.2	75.4	66.5	75.4	69.9	196	5.46	1500	670	1159	+4.9
24	232	80.0	73.5	73.4	76.0	67.0	76.0	69.9	198	5.45	1450	660	1150	+3.3
25	227	81.4	74.3	73.9	76.4	66.5	76.4	70.2	150	4.21	1560	647	1105	-1.3
25	195	80.7	74.1	73.7	75.9	67.1	75.9	70.4	135	3.77	1310	577	1159	+4.6
27	183	80.4	74.1	73.8	75.9	67.6	75.9	70.7	145	4.06	1260	524	1170	-1.3
28	162.5	80.2	74.3	73.9	75.8	67.8	75.8	70.9	119	3.33	990	465	1222	+3.2
29	128.5	80.2	73.2	73.7	75.4	66.6	75.4	70.2	128	3.60	850	364	1497	+1.5

TABLE III
Constant Wall Temperature

Run	$\frac{m}{lbm}$ $\frac{hr}{hr}$	t_{bhi} °F	t_{bho} °F	t_{bco} °F	t_{bci} °F	t_a °F	t_{ben} °F	h $\frac{BTU}{hr-ft^2-°F}$	Nu	$\frac{Q}{BTU}$ $\frac{hr}{hr}$	Re	St	Fig. A Temp. Variation %
30	85.5	110.2	108.8	108.5	81.7	105.2	98.6	108	2.89	2256	342	1919	+3.0
31	138.4	107.5	105.1	103.5	78.6	105.3	93.9	132	3.64	3426	534	1445	-15.9
32	131.5	107.5	106.3	102.3	77.3	104.5	93.9	119	3.20	3290	501	1382	+0.0
33	213	104.3	102.1	95.7	74.0	100.0	88.7	154	4.17	4630	719	1272	-5.0
34	253	103.2	99.6	95.9	72.1	100.8	87.6	200	5.42	6030	911	1207	+1.1
35	268	110.4	106.0	93.5	69.8	103.1	86.1	208	5.63	6080	965	1185	+3.8
36	300	105.2	103.2	92.6	71.8	102.1	87.2	201	5.46	6300	1078	1100	-0.3
37	475	99.9	94.1	89.3	66.8	96.4	83.0	254	6.93	10700	1645	846	+0.9
38	835	101.6	94.2	83.6	63.6	94.5	76.3	450	12.3	16700	2690	815	-0.2
39	570	106.1	101.9	86.7	64.6	99.4	78.8	315	8.65	12590	1890	830	-0.3
40	695	111.3	104.9	95.1	78.6	105.4	85.6	356	9.70	11480	2520	870	+0.2
41	500	113.2	106.4	93.0	67.8	105.7	83.8	258	7.0	12600	1760	926	+0.8
42	389	105.6	100.8	92.3	68.6	100.6	94.3	246	6.68	9210	1360	1104	+0.9
43	170	102.0	99.8	92.8	71.6	97.5	86.2	159	4.37	3600	578	1518	+1.6
44	120	99.1	97.3	93.8	78.3	96.3	83.8	123	3.34	1860	426	1735	+1.6
45	87.5	98.8	97.6	96.2	81.2	97.5	90.7	96.8	2.71	1310	321	1945	-0.1
46	65.0	104.3	103.3	98.0	82.5	100.9	92.7	76.3	2.15	1010	242	2260	+1.6

SKETCH OF HEAT EXCHANGER

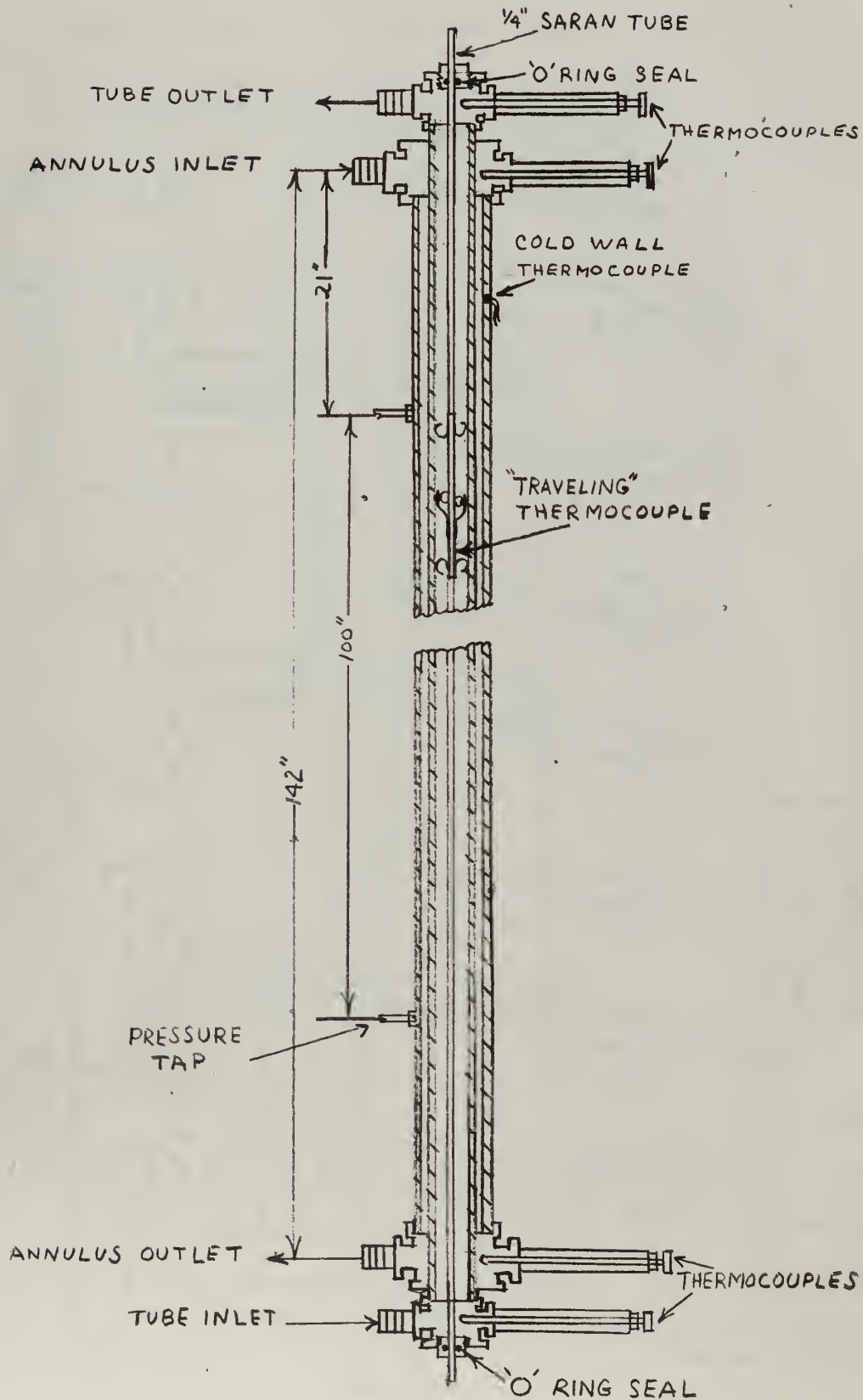
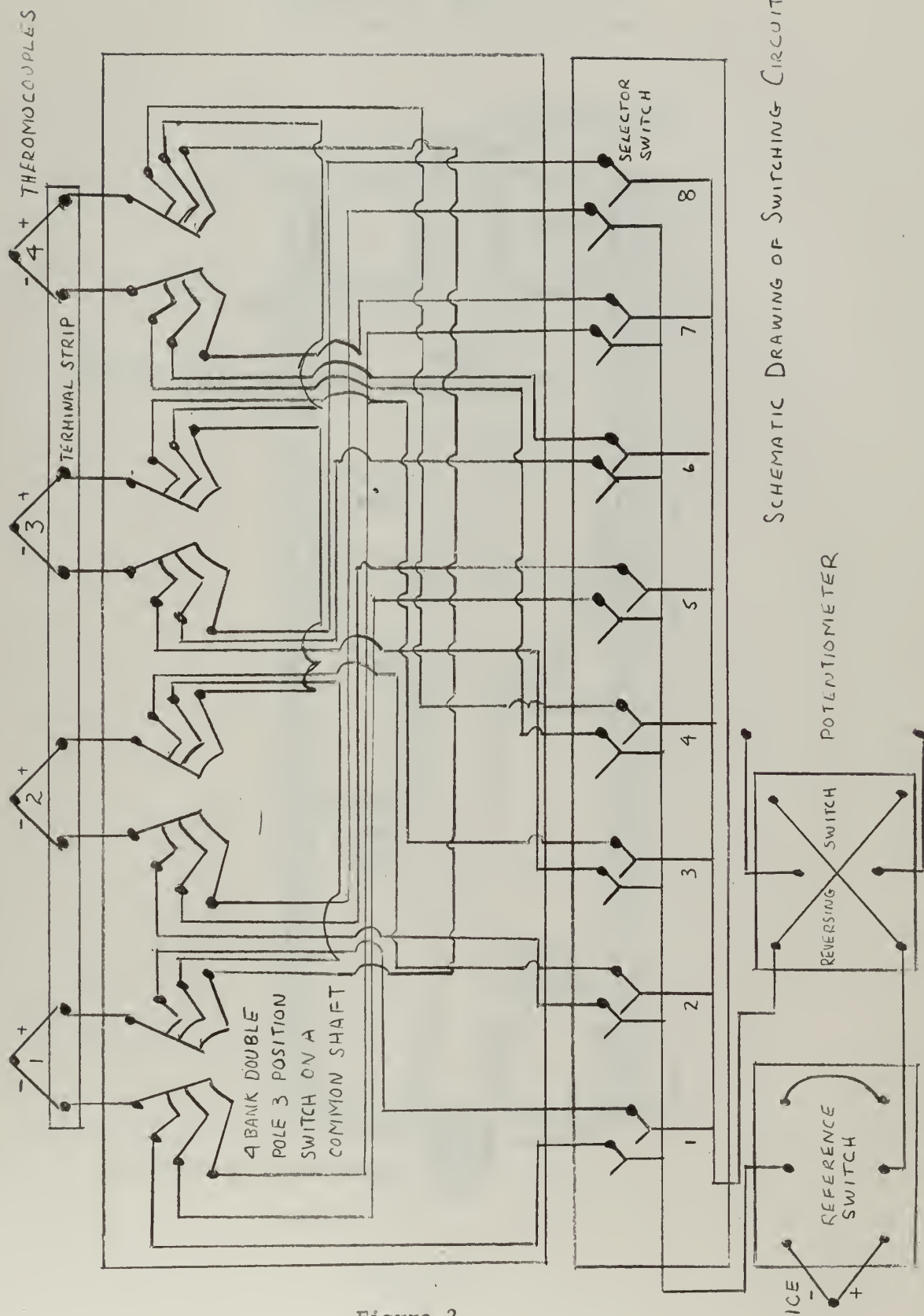


Figure 1



SCHEMATIC DRAWING OF SWITCHING CIRCUIT

Figure 2

SCHEMATIC DRAWING OF "TRAVELING" THERMOCOUPLE

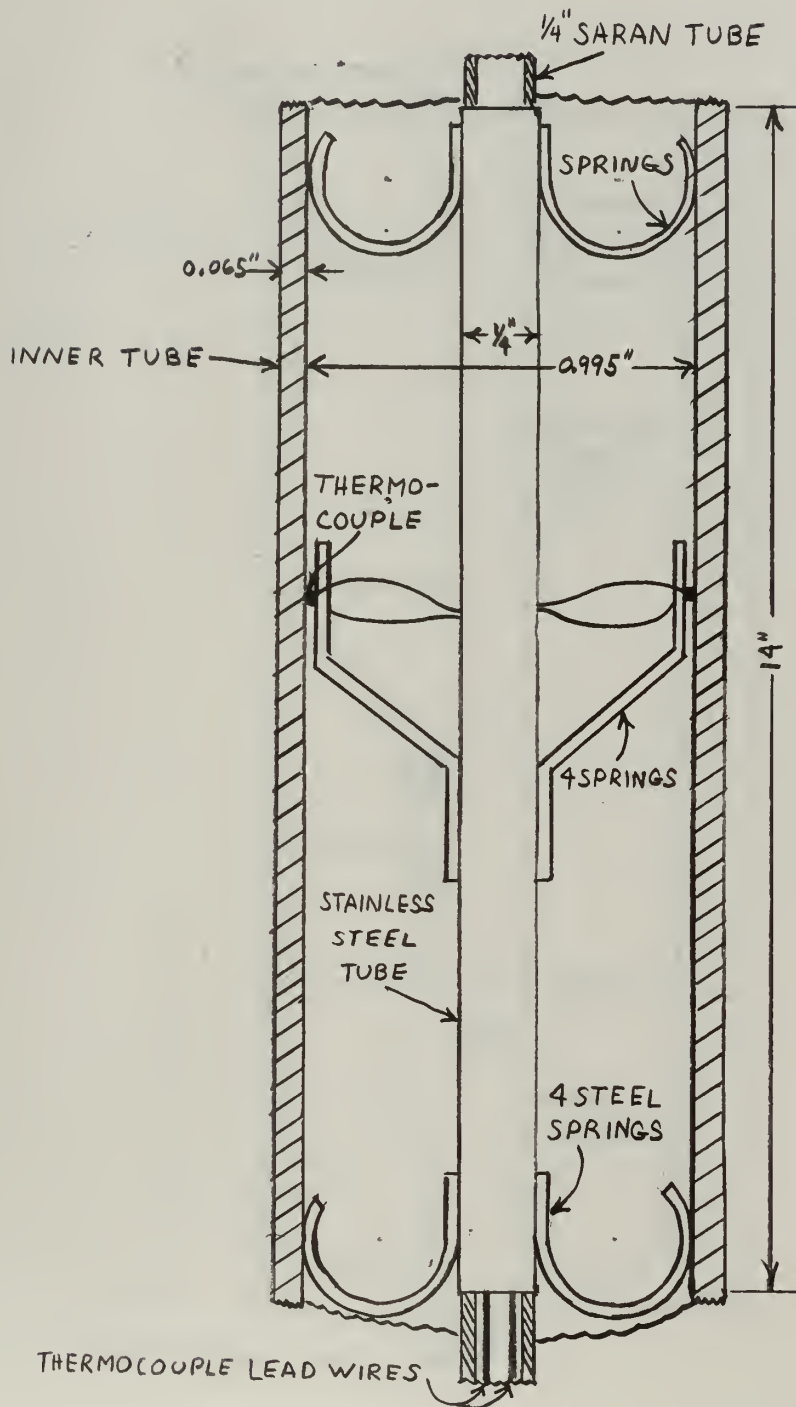


Figure 3

SCHEMATIC DRAWING OF "TRAVELING" THERMISTOR

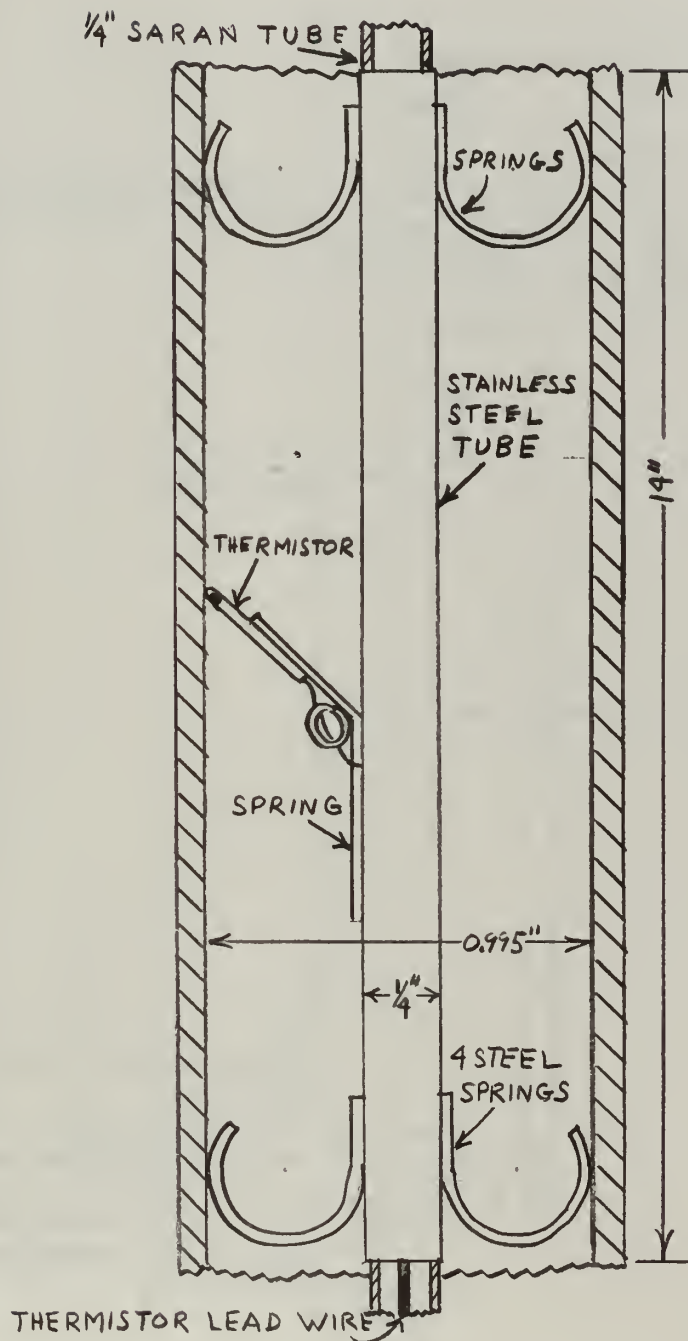


Figure 4

SCHEMATIC ARRANGEMENT OF EQUIPMENT

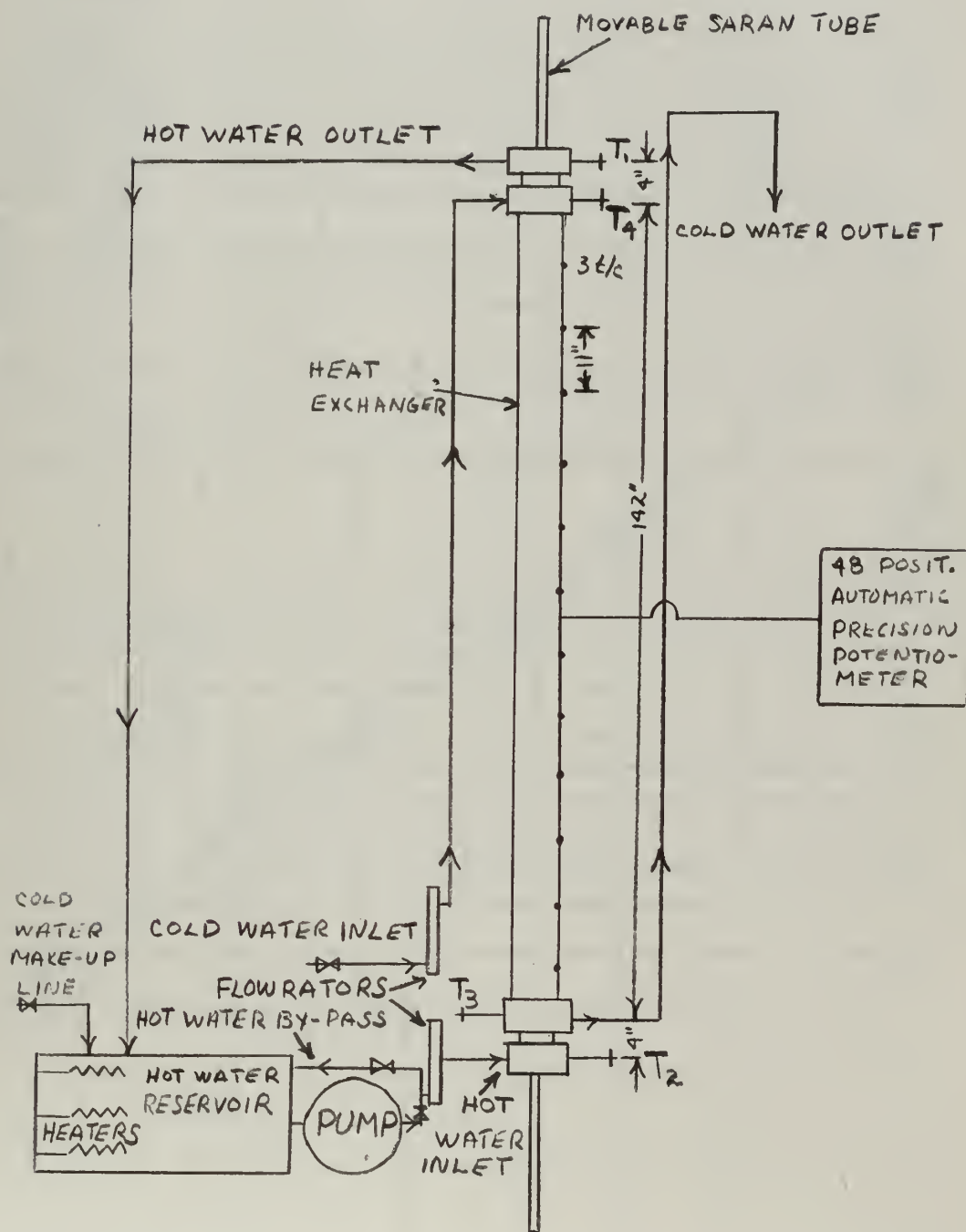


Figure 5

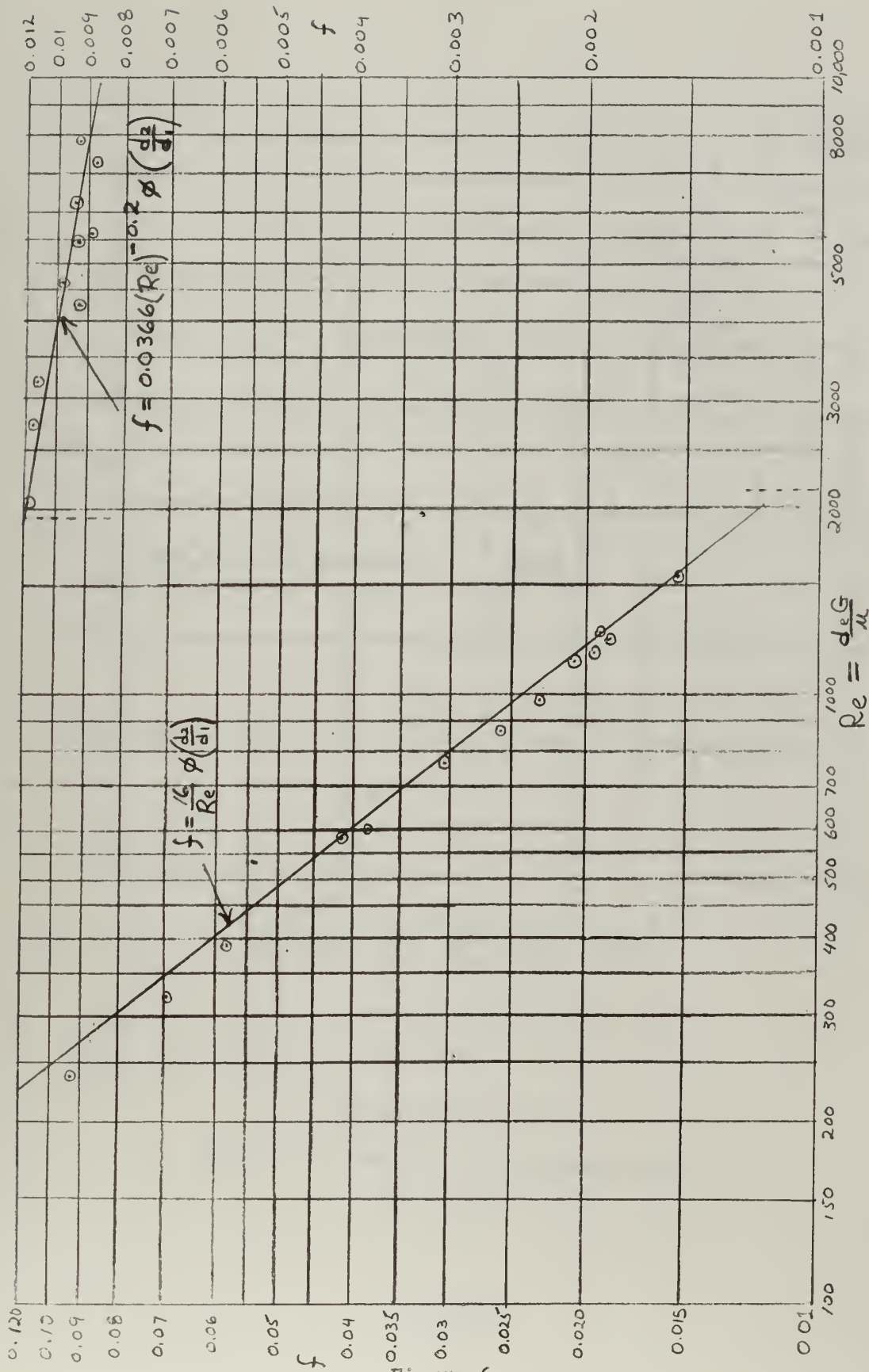
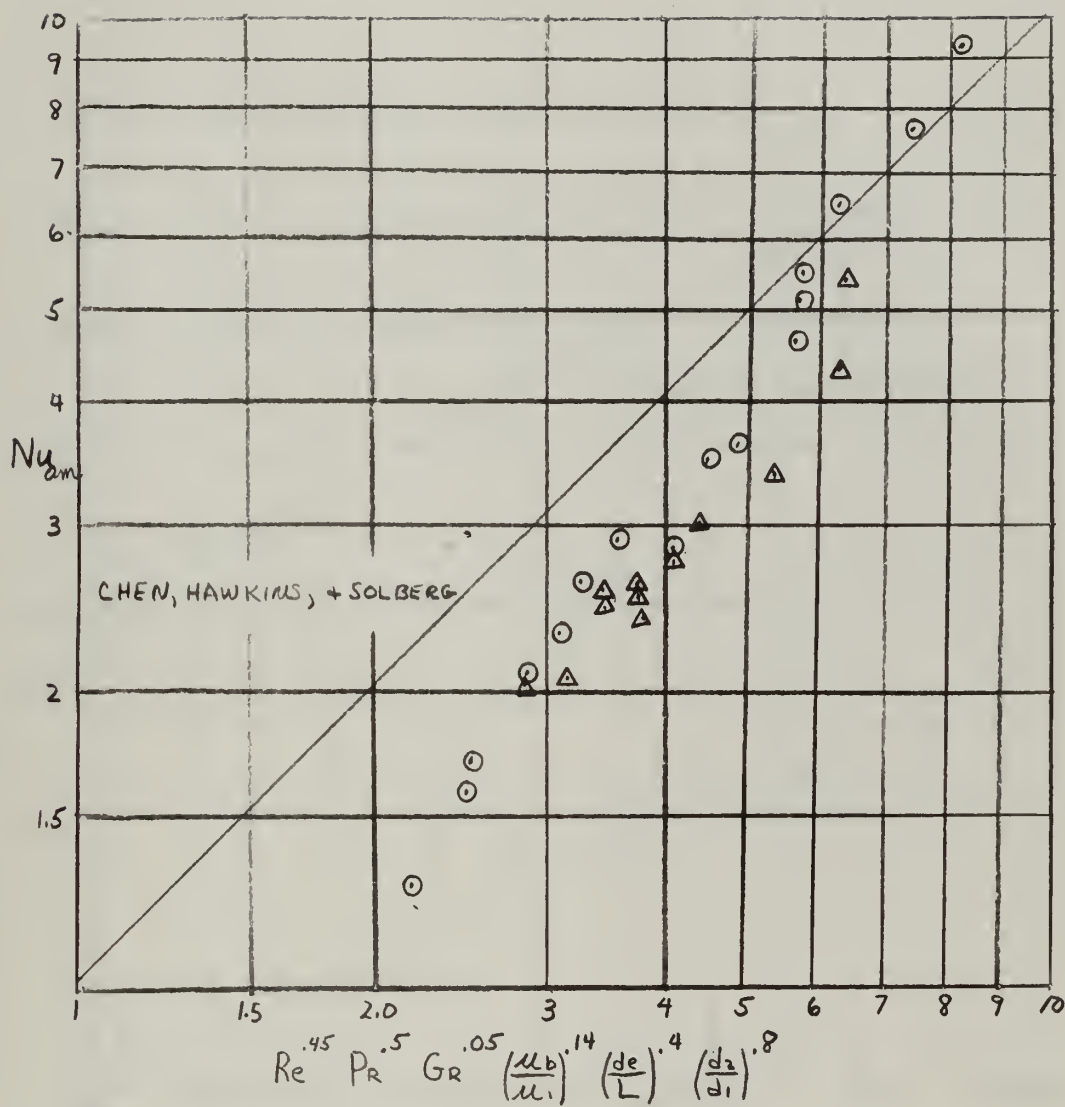


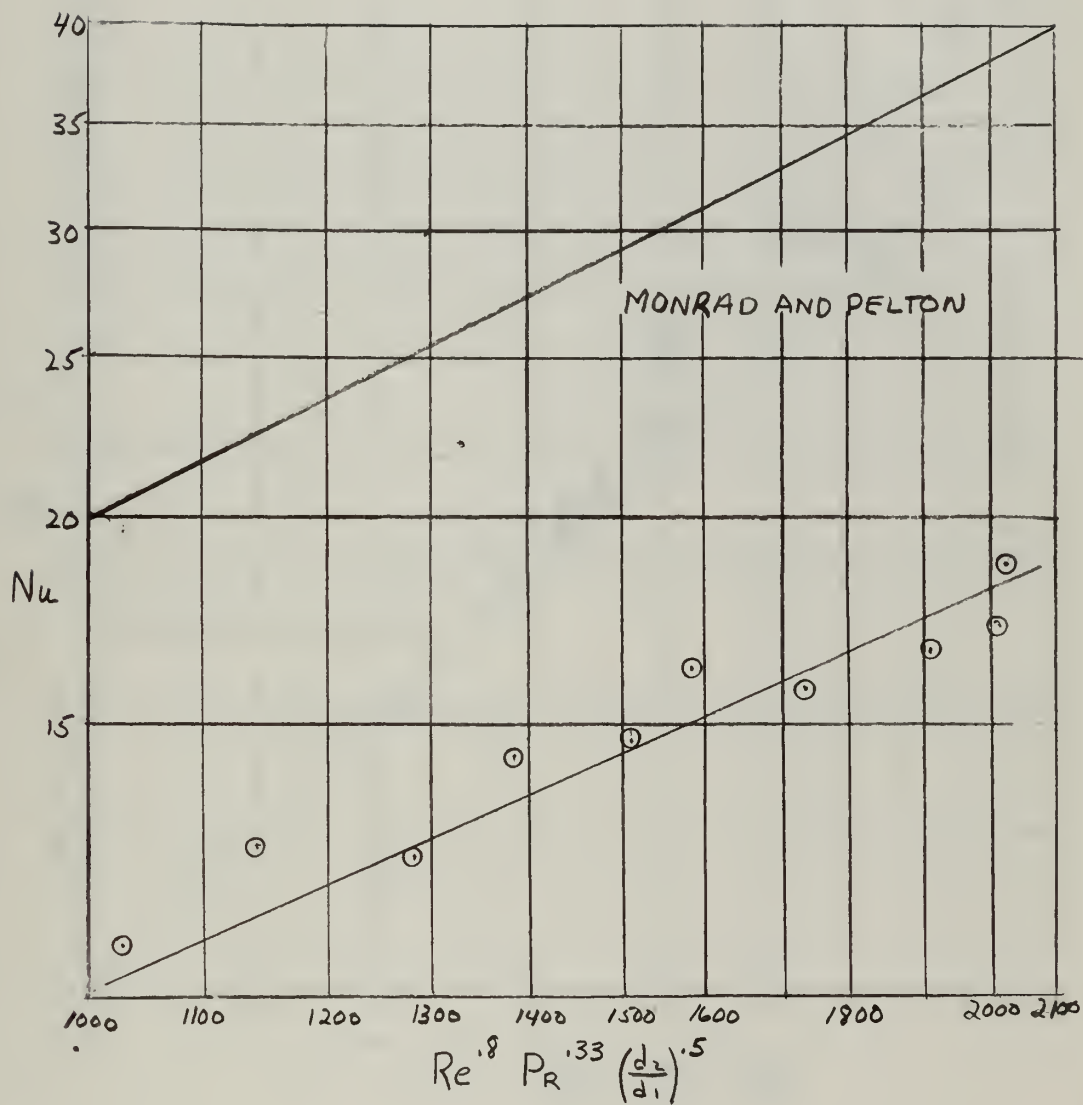
Figure 6

ISOTHERMAL FRICTION DATA



Laminar Flow Runs
 based on arithmetic bulk temperatures.

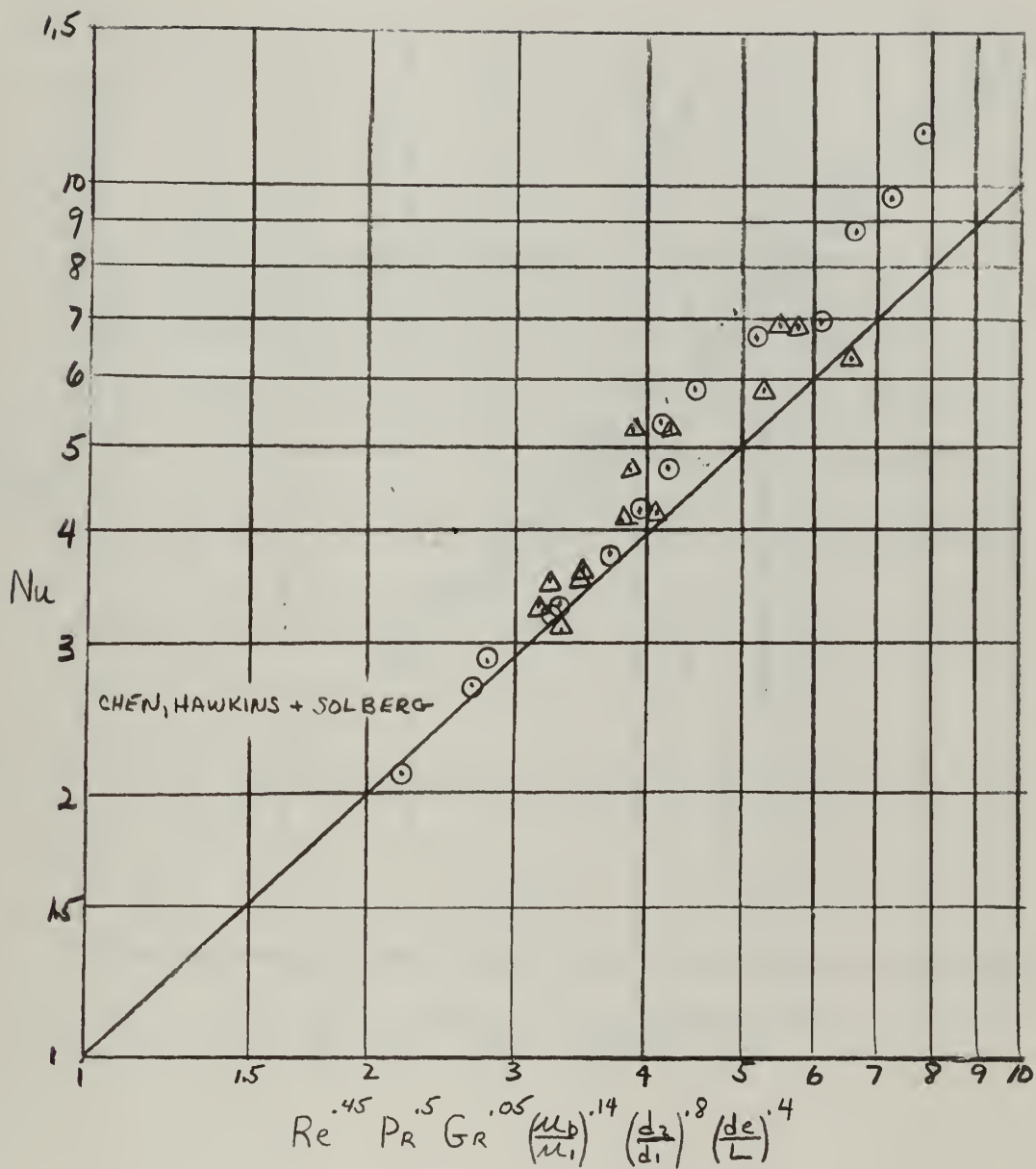
Figure 7



Turbulent Flow Runs

Based on average bulk temperatures.

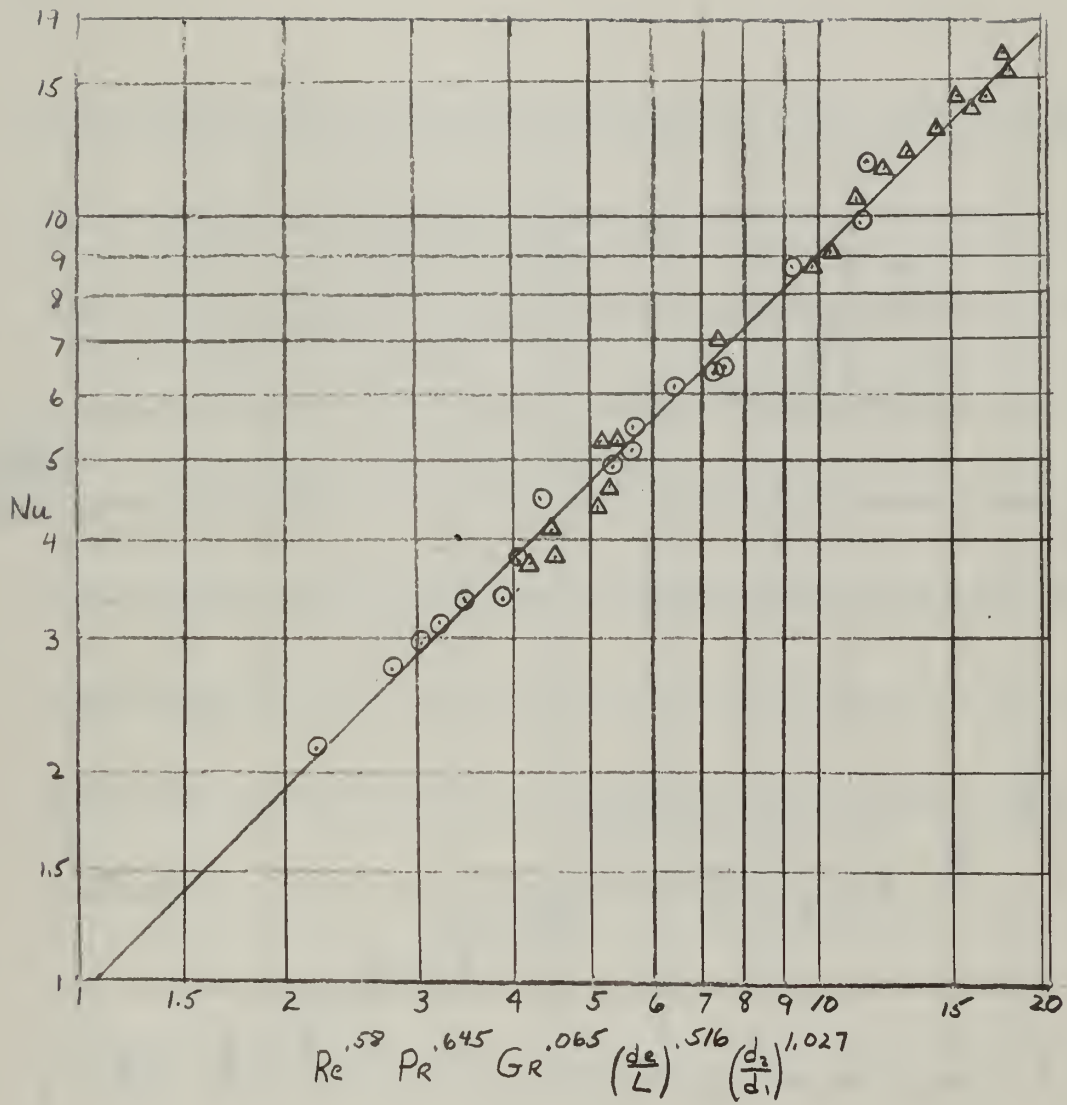
Figure 8



Laminar Flow Runs

Based on average bulk temperature with fluid properties based on average film temperature.

Figure 9

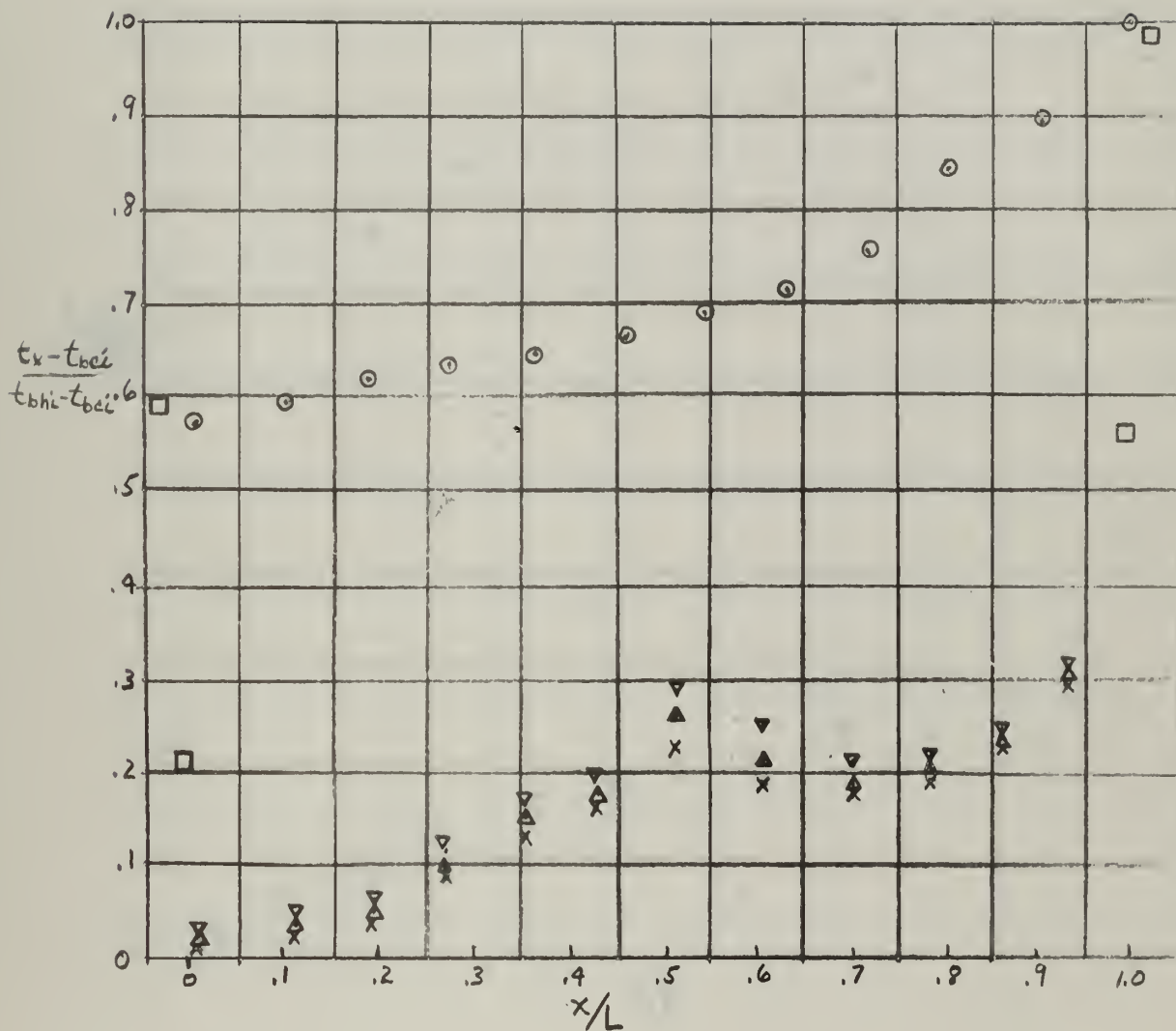


All Runs

Based on average bulk temperature and fluid properties based on average film temperature.

Figure 10

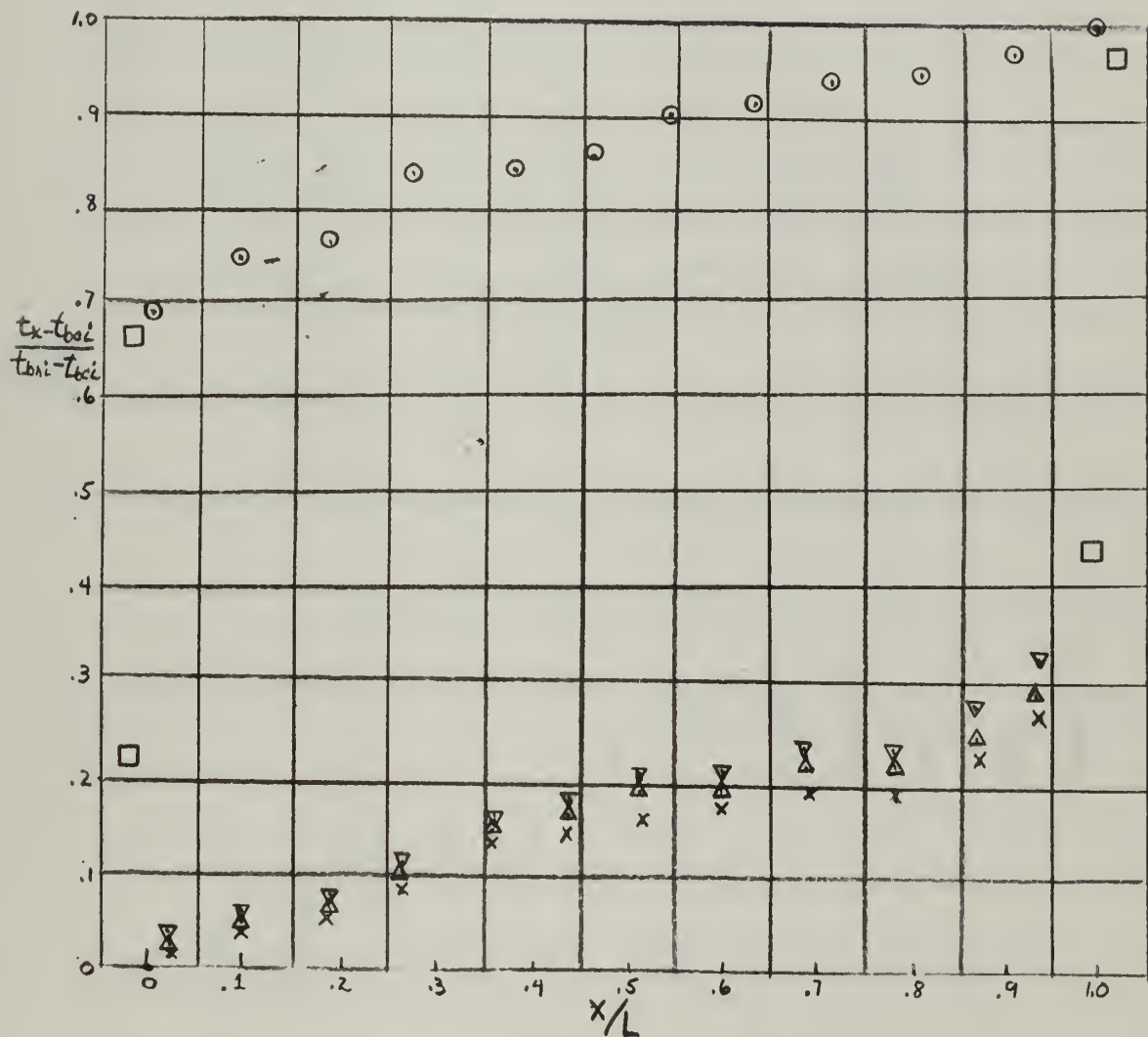
- Bulk temperature
- Inner wall temperature
- X } - Outer wall temperature
- △ } - Outer wall temperature
- ▽ } - Outer wall temperature



Dimensionless plot of temperature versus annulus length for run 7.

Figure 11

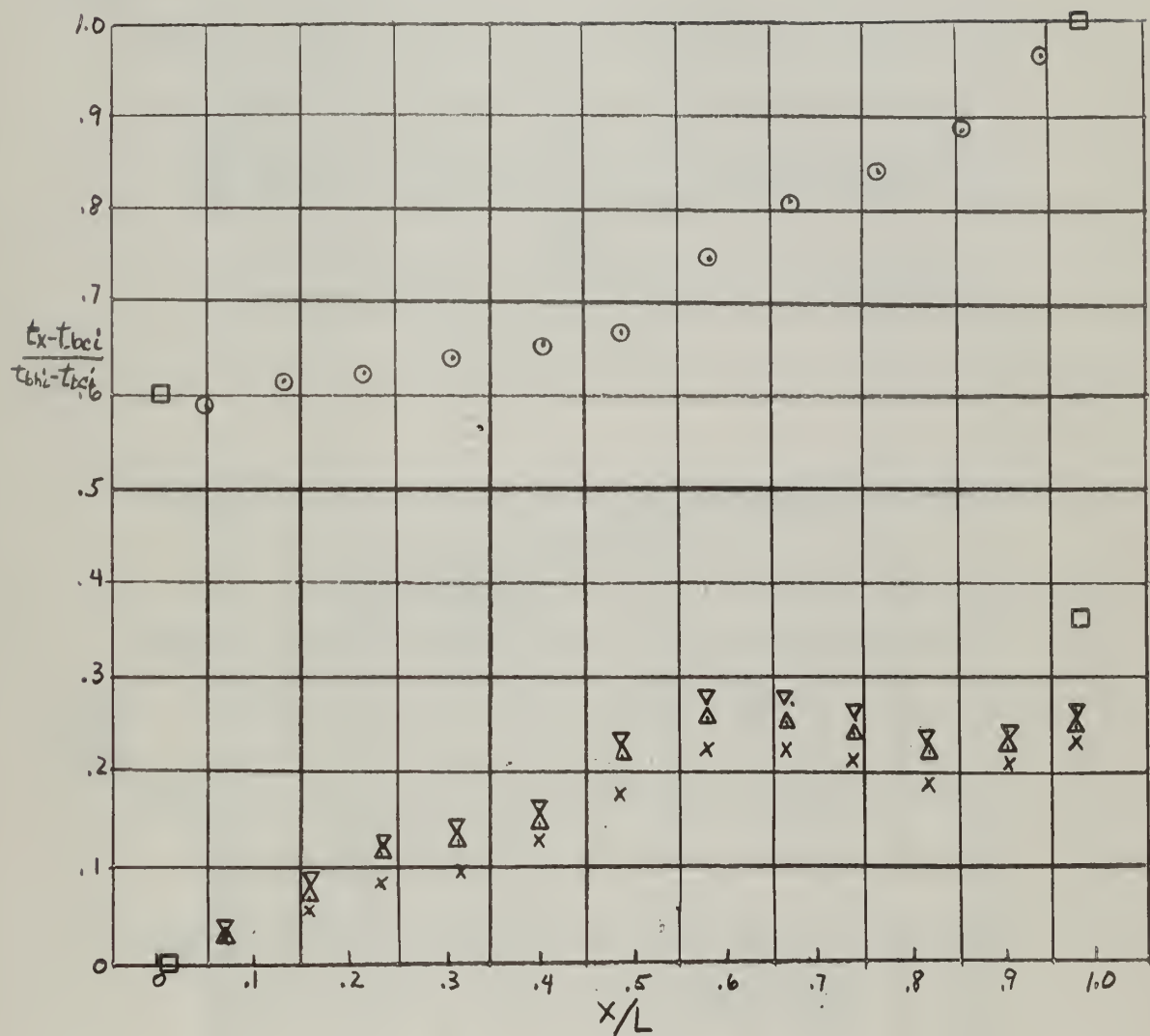
- Bulk temperature
- Inner wall temperature
- x } - Outer wall temperature
- △
- ▽



Dimensionless plot of temperature versus annulus length for run 20.

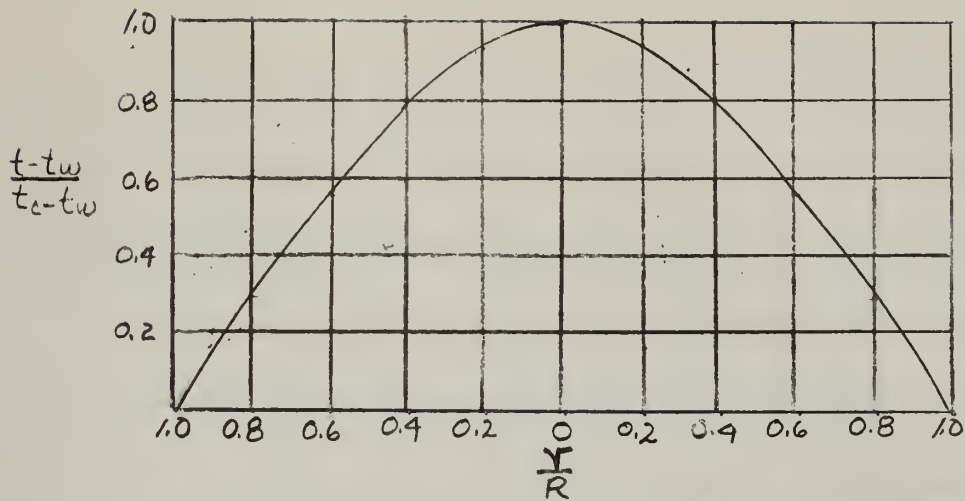
Figure 12

- Bulk temperature
- Inner wall temperature
- x } Outer wall temperature
- △ } Outer wall temperature
- ▽ } Outer wall temperature



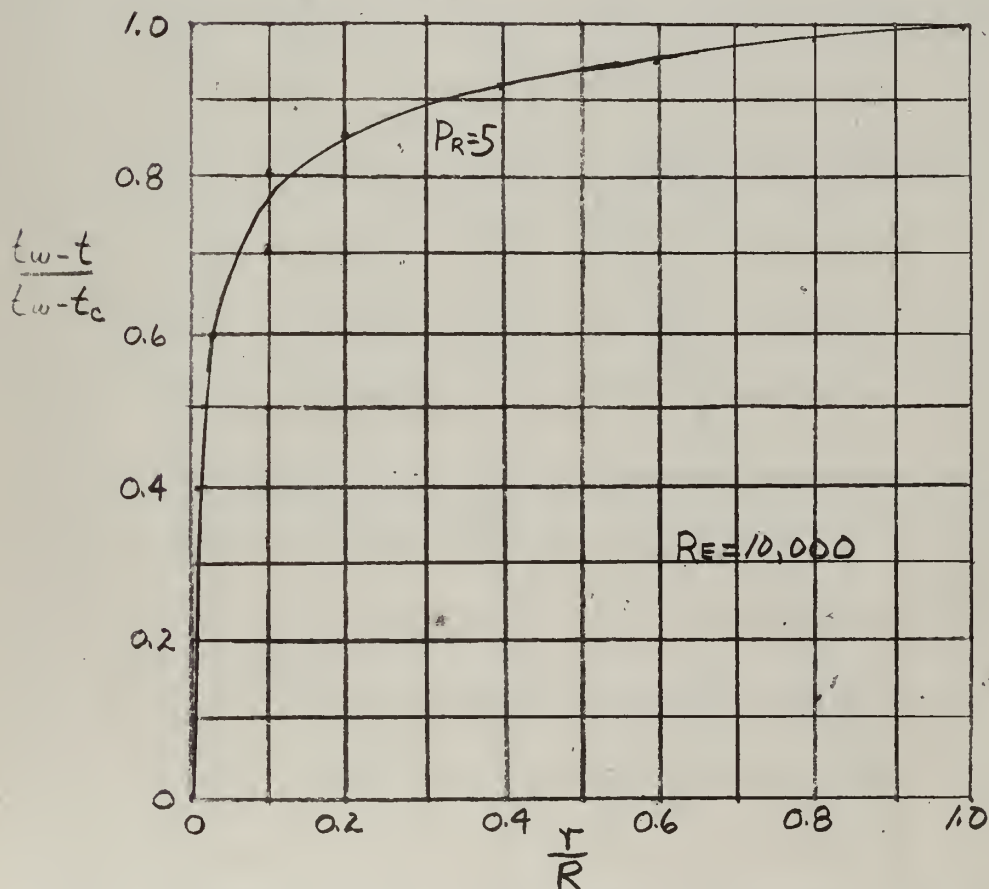
Dimensionless plot of temperature versus annulus length for run 28.

Figure 13



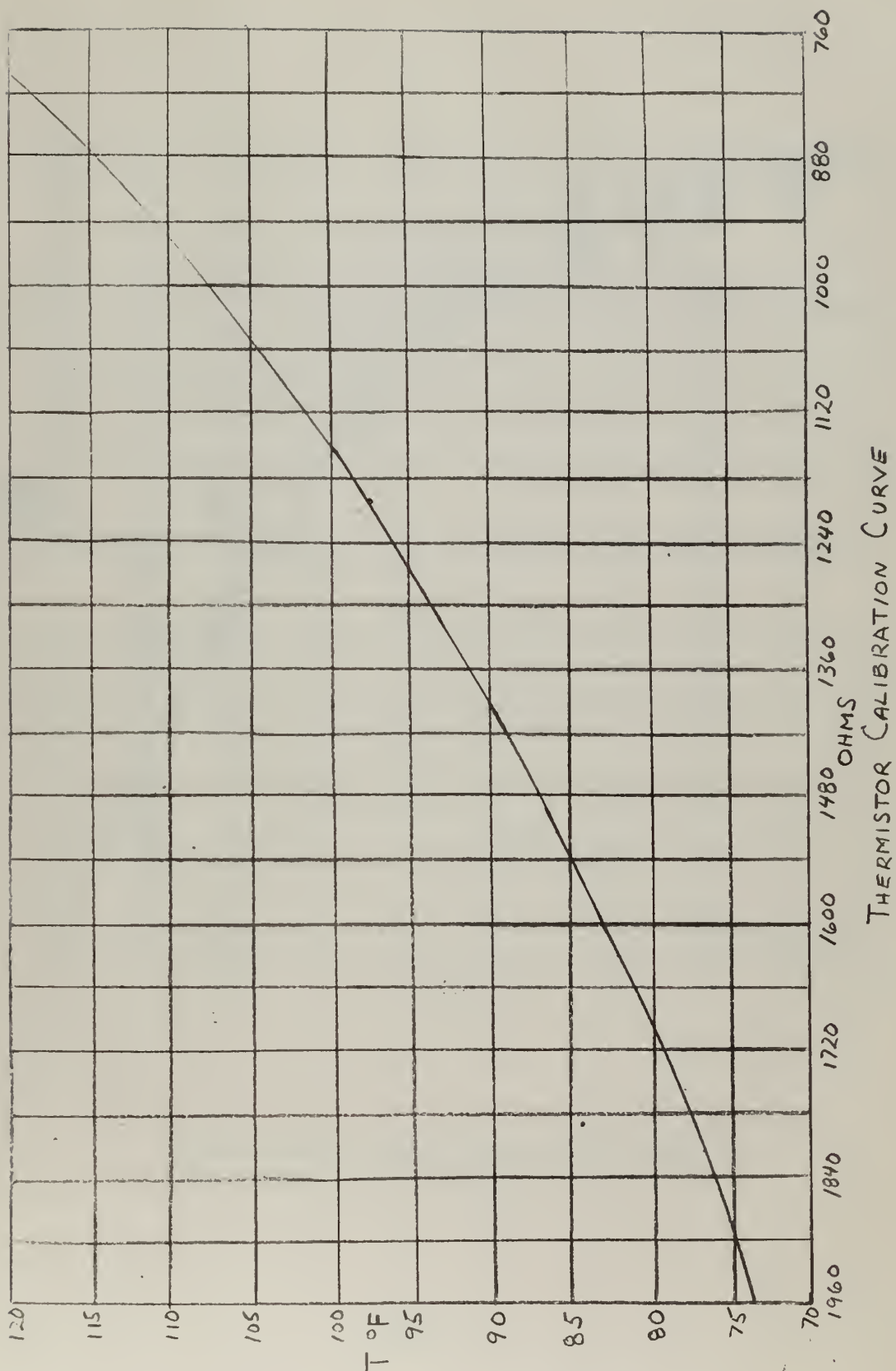
LAMINAR TEMPERATURE PROFILE IN A TUBE, [9]

FIGURE 14a



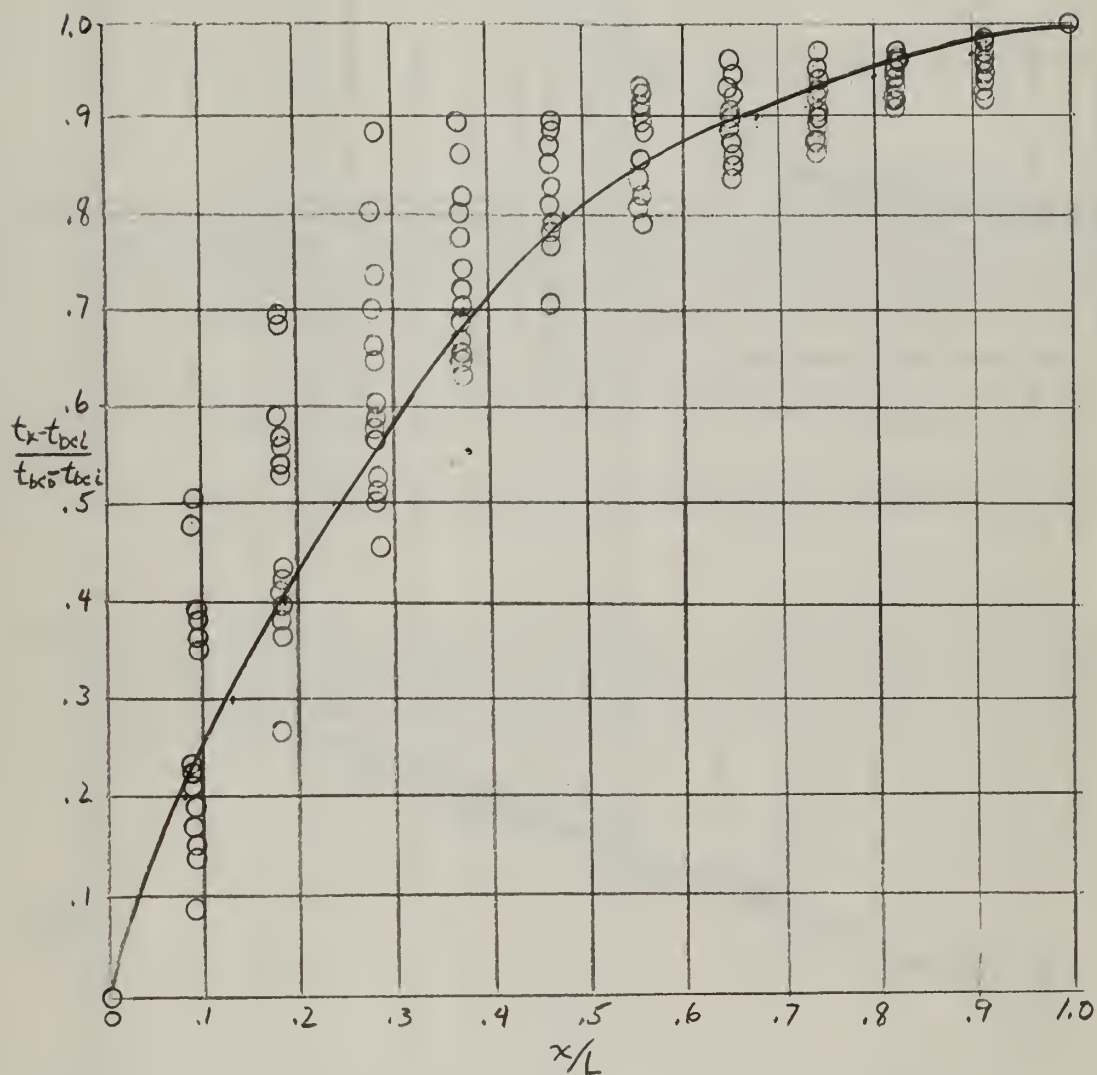
FULLY DEVELOPED TEMPERATURE DISTRIBUTION IN A CIRCULAR PIPE, [10]

FIGURE 14b



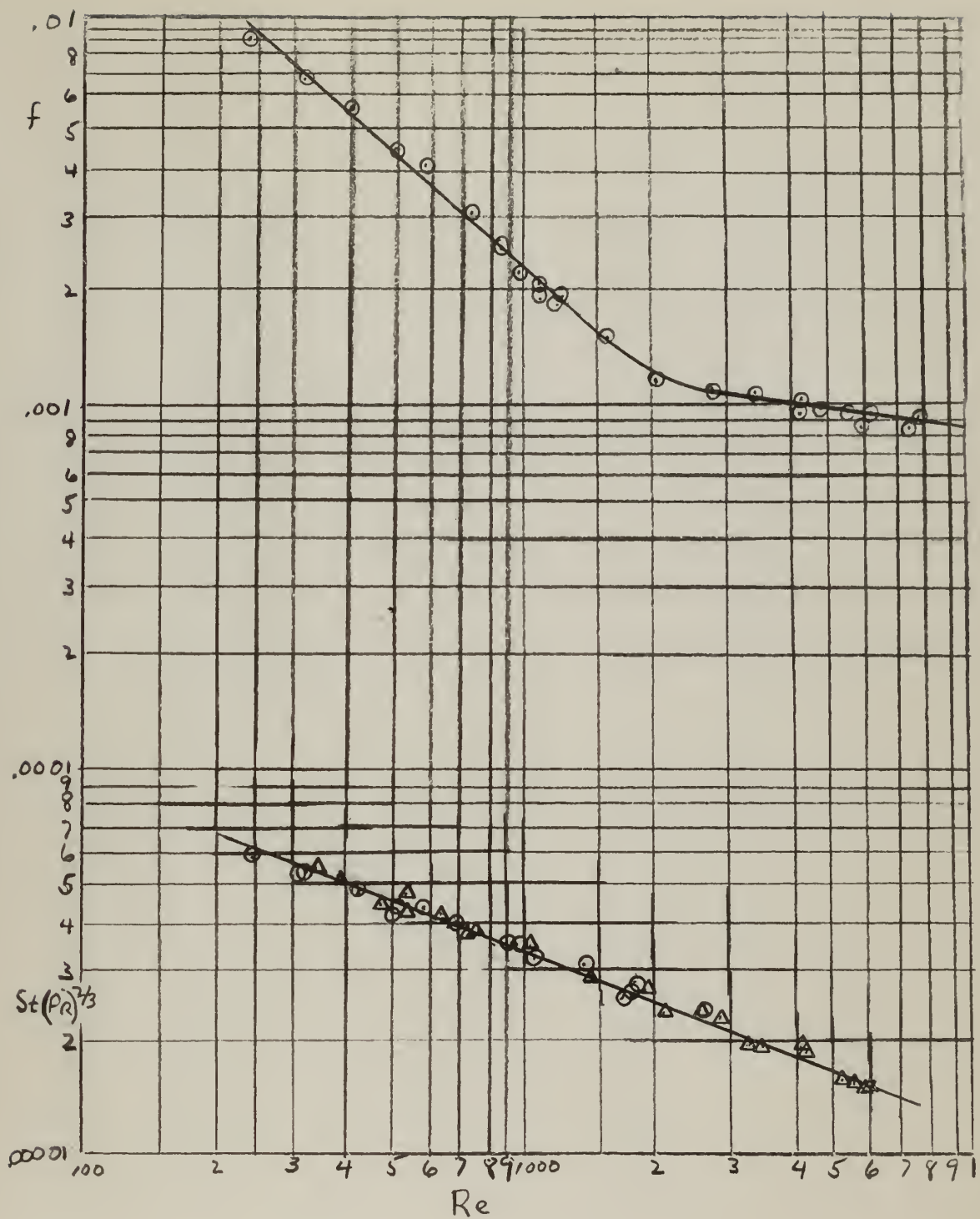
Calibration curve for the thermistor.

Figure 15



Dimensionless temperature versus length for the constant wall temperature runs.

Figure 16

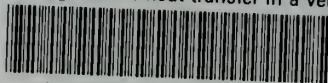


f and $St(Pr)^{2/3}$ versus Re .

Figure 17

thesB8855

Investigation of heat transfer in a vert



3 2768 002 08810 6

DUDLEY KNOX LIBRARY